RESEARCH ARTICLE

Wearable Multimodal Optical Analyzers: Physiological Variability and Reproducibility of Measurements

Yu. I. Loktionova[1] | E. V. Zharkikh[1] | V. E. Parshakova[1] | V. V. Sidorov[2] | A. V. Dunaev[1]

[1]Research and Development Center of Biomedical Photonics, Orel State University, Orel, Russia | [2]SPE "LAZMA" Ltd, Moscow, Russia

Correspondence: A. V. Dunaev (dunaev@bmecenter.ru)

Received: 26 November 2024 | **Revised:** 18 December 2024 | **Accepted:** 22 December 2024

Funding: This work was supported by Russian Science Foundation (project no. 23-25-00522).

Keywords: blood microcirculation | coefficient of variation | fluorescence spectroscopy | laser Doppler flowmetry | microcirculatory-tissue system | physiological variability | reproducibility | wearable multimodal analyzers

ABSTRACT

The work is devoted to the study of the physiological variability of the microcirculatory-tissue system (MTS) parameters under normal conditions and during functional tests. The results were obtained in vivo using multimodal wearable analyzers implementing methods of laser Doppler flowmetry and fluorescence spectroscopy. Comprehensive data analysis and calculation of the coefficients of variation of the MTS parameters of the human body for various topographic and anatomical areas of the skin were carried out. The obtained results showed higher values of the coefficient of variation of MTS parameters in the area of the toes and wrists, while the fingers and forehead skin showed lower levers of variation. In all areas of the study, reproducibility of the parameters obtained for the right and left areas of the study is observed.

1 | Introduction

The microcirculatory-tissue system (MTS) is a structural and functional unit of organs and biological tissues, consisting of vessels of the microcirculation bed, cellular biological tissue, lymphatic microvessels, and nerve endings. The MTS is responsible for the exchange of oxygen and nutrients between the blood and cells in biotissues, and is the first link in the development of pathological conditions and structural disorders in the vascular system [1–4]. Therefore, the diagnosis of the MTS is an important criterion for diagnosis.

However, the functional state of MTS is subject to change due to various factors. Firstly, the microcirculatory bed has anatomical heterogeneity. For instance, the skin of the palm surface of the hands and the plantar surface of the legs (apical skin areas) contains a large number of arterio-venular anastomoses (AVA), whereas in the nonapical skin areas (skin of the face, dorsal side of the arms, etc.) there are practically no AVA. Such anatomical differences determine the peculiarities of MTS functioning. The difficulty of an adequate assessment of the functional state of MTS is associated with the high variability of their parameters. MTS parameters can change for the same person during the day, week, or month. The heterogeneity of the blood microcirculation system state can be influenced by various factors, which include age, sex, anatomical measurement site, physical and mental activity, body and indoor air temperature, food intake, and so forth.

Age-related changes are one of the most important factors leading to individual variability in MTS parameters. With age, functional changes in all body systems occur in the human body [5], including the cardiovascular system [6, 7]. At the microcirculatory level, age-related changes include a decrease in the density of the capillary network [8, 9] accompanied by an increase in vascular length [10], impaired microvascular reactivity and increased arterial stiffness [11, 12], which leads to an increase in skin perfusion in zones with glabrous skin [13]. It is worth noting that age-related changes in the microcirculatory bed of skeletal muscles become more pronounced with physical exertion,

which may be associated with a decrease in vasodilator capacity and a decrease in capillarization [14].

The ambient temperature has a significant effect on blood microcirculation. It was shown [15, 16] that the microcirculatory bed not only reacts to changes in room temperature but also participates in the thermoregulation of the body itself. Local heating and cooling also cause a local change in microcirculation, such as vasodilation with an increase in blood flow intensity [17, 18] and vasoconstrictor changes [19]. Accordingly, it is actively used as a functional test for the diagnosis of microcirculatory disorders [20].

The rheological properties of blood also affect the microcirculation [21]. For example, the work [22] shows the relationship between erythrocyte deformability and homeostasis, as well as local tissue metabolism and oxidative stress.

The authors [23] note that continuous aerobic exercise improves vascular endothelial function. High-intensity interval exercise increases brachial artery expansion and enhances peripheral blood flow in the skin and retina [24]. Microcirculation changes after physical activity depend on initial blood flow levels: it increases in those with initially low levels and decreases in those with higher levels, reflecting activation of regulatory mechanisms [25].

Healthy people with high levels of daily psychological stress have greater vasoconstriction compared to healthy people with lower stress levels [26]. An increase in myogenic oscillations is observed with a relatively stable intensity of low-frequency fluctuations in microcirculation under stress conditions [27]. Other researchers also report an increase in endothelial activity against the background of decreased sympathetic adrenergic activities [28]. It was also shown that a high level of stress leads to the development of endothelial dysfunction [29].

Smoking causes morphological and functional changes in microvessels, leading to the development of blood microcirculation disorders, including impaired endothelium-dependent vasorelaxation and platelet aggregation [30, 31]. A slower recovery phase after smoking a cigarette in smokers suggests that their microcirculation gets used to smoking [32–34]. However, even passive smoking leads to changes in blood microcirculation, causing a delay in oxygen consumption by peripheral tissues [35]. In addition to smoking, alcohol and opioid use lead to pathophysiological changes in coronary microcirculation, which is a predictor of coronary heart disease and thrombosis [36, 37].

Researchers highlight the effect of circadian rhythms on the cardiovascular system [38–40], particularly blood pressure, peripheral resistance [41], and cutaneous blood flow levels [42]. Circadian clocks also influence diurnal metabolic changes [43]. Cerebral perfusion monitoring shows circadian blood flow regulation in this region, independent of blood pressure and motor activity changes [44]. Disrupted circadian rhythms contribute to microvascular pathologies [45], such as night shift work impairing cerebral microcirculation [46], and increased photoperiods disrupting microvascular blood flow regulation, reducing endothelial, neurogenic, and myogenic oscillations, and lowering tissue perfusion [47]. Night sleep quality also affects cutaneous microcirculation. Patients with severe obstructive sleep apnea experience nocturnal blood flow reductions, increased heterogeneity [48], and related pathology risks [49].

Also, changes in blood microcirculation are caused by various functional tests, for example, occlusion, local heating and cooling, as well as the use of pharmacological substances [50]. General anesthesia reduces the oscillatory components of the perfusion signal associated with sympathetic, myogenic activity and the endothelial modulated component [51].

Men and women have some differences in peripheral blood flow, which is due to several factors [52, 53]. The thickness of men's skin is greater than that of women's, while the thickness of subcutaneous fat in women is greater [54]. Higher levels of sebum secretion are observed in men compared to that of women [55]. Differences between men and women of reproductive age were observed, including menstrual cycle phases in women: basal blood flow was lowest in the luteal phase and highest in the preovulatory phase, with the greatest reduction in finger skin perfusion during cooling and the slowest recovery afterward [56]. Additionally, vasodilation from local heating occurred at a lower skin temperature in women compared to men [57].

Numerous factors influence oxidative metabolism in the human body, such as sex, age, the presence of pathologies, the menstrual cycle phase in women, levels of physical activity, and nutrition. Let us examine some of these in more detail.

First and foremost, the basal metabolic rate of the human body decreases with age [58]. In the another work [59], it was shown that oxidative DNA damage occurring during aging leads to hyperactivation of PARP proteins, which depletes NAD+ reserves and limits energy production in cells. The basal metabolic rate of the human body also depends on sex, as well as the muscle and fat mass and their ratio [60]. The authors [61] demonstrated that fat mass exerts a greater influence among the listed factors in both men and women. The menstrual cycle in women causes hormonal fluctuations, which, in turn, trigger a cascade of reactions across all body systems, including changes in the metabolism of biological tissues [62]. Performing physical exercise activates oxidative metabolism in muscle cells and increases cellular oxygen consumption [63].

Figure 1 shows the main factors that influence the microcirculatory-tissue systems of the human body.

Optical non-invasive diagnostic methods are employed to assess the MTS parameters. One of the advantages of optical methods is the possibility of noninvasive assessment of the condition of the capillary segment of the cardiovascular system, which is the first link in the chain of functional disorders in various socially significant diseases leading to pathologies of larger vessels and the circulatory system as a whole. Examples of such methods are laser Doppler flowmetry (LDF) and fluorescence spectroscopy (FS).

The use of the laser Doppler technique for blood flow measurements was first reported by Riva et al. [64] studying retinal flow in rabbits and Stern studying skin blood flow in humans [65]. The LDF method is based on probing tissues with laser

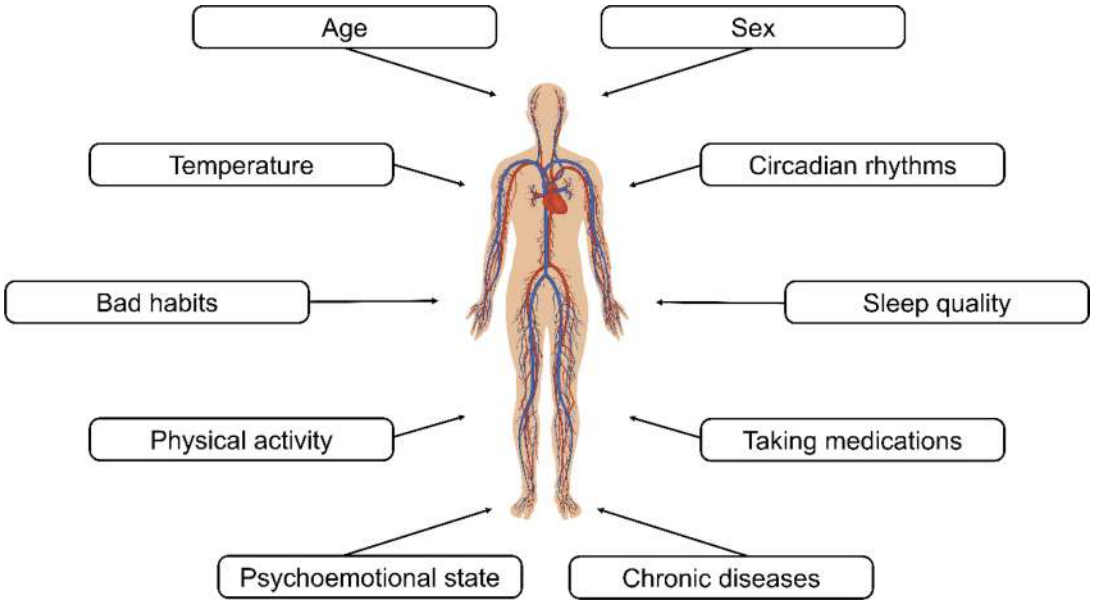

FIGURE 1 | Factors affecting the state of microcirculatory-tissue systems.

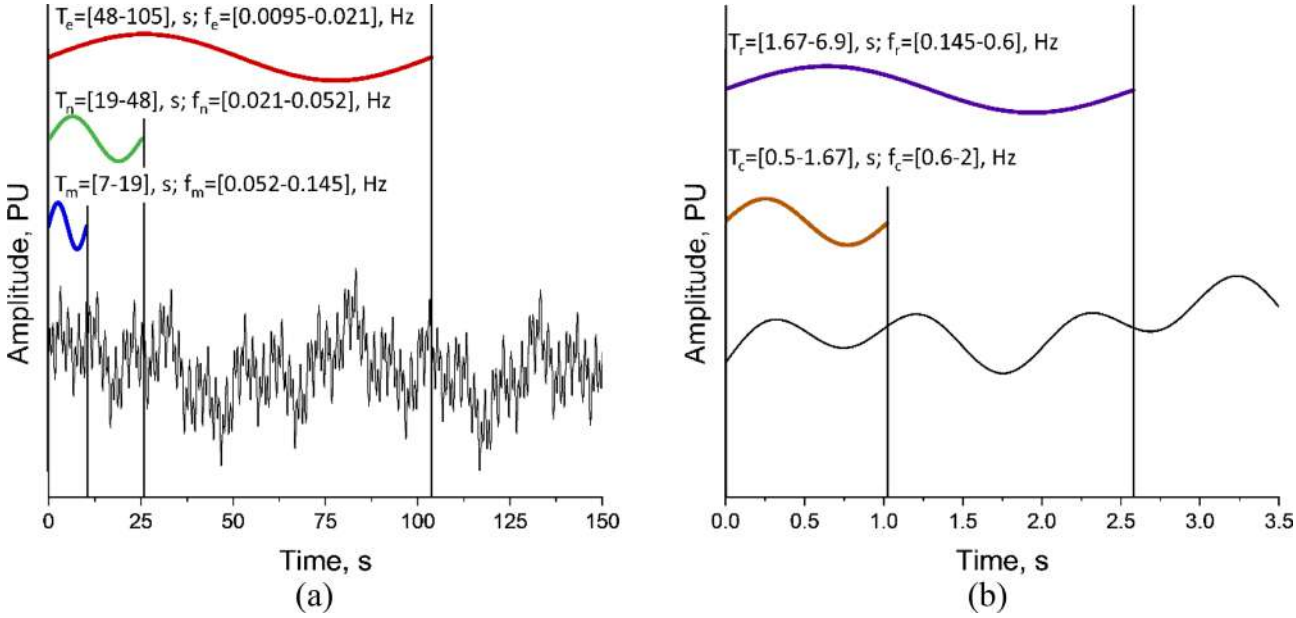

FIGURE 2 | Schematic representation of fluctuations of active (a) and passive (b) mechanisms of blood flow regulation: Endothelial (red), neurogenic (green), myogenic (blue), respiratory (purple), cardiac (brown).

radiation and analyzing the scattered component of the light reflected from moving red blood cells. When coherent radiation from a laser source enters biological tissue, it is scattered and partially absorbed. Laser radiation reflected from static tissue components does not change its frequency, while laser radiation reflected from moving particles (erythrocytes) is characterized by a frequency shift in accordance with the Doppler effect. The magnitude of the recorded LDF signal depends on the concentration of erythrocytes in the probed volume of biological tissue and the average speed of their movement. The perfusion signal recorded by the LDF method has a complex structure consisting of the superposition of several oscillatory components. The analysis of LDF fluctuations allows one to further study the mechanisms of regulation of microcirculatory blood flow in a wide range of frequencies (from 0.0095 to 2 Hz) [66, 67].

Figure 2 shows an example of five oscillatory components when they are superimposed on a total tissue perfusion signal.

The FS method is based on the use of optical radiation with a wavelength in the ultraviolet or visible spectral region to irradiate biological tissue and record autofluorescence spectra of endogenous and exogenous fluorophores [68, 69]. Biological tissues contain a variety of natural endogenous fluorophores with different characteristics, such as absorption and emission in different spectral regions, quantum yield and fluorescence lifetime. The total autofluorescence signal depends on the number and spatial distribution of fluorophores in biological tissue, as well as on its metabolic status and morphology in normal and pathological conditions. Among the substances, that exhibit the most vivid autofluorescence in biological tissues, can be distinguished

NADH and FAD coenzymes, structural proteins, such as collagen and elastin, amino acids—tryptophan and tyrosine, as well as porphyrin, lipofuscins and melanin [70].

Various manufacturers provide equipment for registering microcirculatory-tissue systems parameters, including Perimed AB, LAZMA Ltd., Transonic Systems Inc., Moor Instruments Ltd., Oxford Optronix Ltd., and LEA Medizintechnik [71]. The main technical characteristics of the equipment implementing the LDF method are given in Table 1.

Varied modifications of devices from one manufacturer (e.g., Perimed AB) have different technical characteristics, that affect the recorded parameters values. Stationary devices with a Periflux PER TV and Periflux PER 3 fiber optic probes use a Helium-Neon laser with a wavelength of 632.8 nm and a power of 2 mW as an emitter. New modifications Periflux System 5000 and PeriFlux 6000 ELOS system use a laser diode with a wavelength of 780 nm as a radiation source. The distance between the signal source and receiver in a fiber optic probe varies from 0.15 to 1.2 mm, the most common value is 0.25 mm. At the same time, it is known that both the wavelength and the distance between the source and the detector affect the depth of penetration and the overall diagnostic volume, that is, devices register microcirculation parameters from different anatomical structures.

In addition to technical equipment, skin optical parameters also affect the recorded signal [78–81]. For example, tissue blood volume and melanin content were identified as key factors influencing FS measurement variability [82]. Stationary instruments with optical fibers can introduce inaccuracies due to difficulties in maintaining consistent conditions during installation and attachment to tissue. Recently, there has been a shift towards miniaturized, user-friendly diagnostic devices, moving away from bulky fiber-optic systems. Eliminating optical fiber probes reduces artifacts during data acquisition, while wireless systems enable comprehensive, long-term monitoring and transmission of diagnostic information, driving advancements in medical diagnostics.

This work is devoted to the study of the physiological variability of MTS parameters using new multimodal wearable analyzers. Previous studies of the physiological variability of LDF and FS signals were performed using stationary devices, like Periflux PF lD [83], Periflux PF3 [84], multifunctional laser non-invasive diagnostic system LAKK-M [82, 85], Periflux 5000 [86] and PeriFlux 6000 EPOS system [87]. This study was conducted using examples of wearable and stationary devices from LAZMA Ltd. with approximately typical technical characteristics for most stationary devices from various manufacturers (Table 1), namely the stationary LAKK-M system and wearable analyzer LAZMA PF [88] (in EU/UK this device is made by Aston Medical Technology Ltd., UK as FED-1b). A comparison of the technical characteristics of wearable devices and a similar system in a stationary version with an optical probe fiber is presented in Table 2.

Wearable analyzers have many advantages over stationary devices. They do not require optical fiber to transfer the recorded signal. This allows for a significant expansion of the possible data recording areas, due to simpler mounting and wireless data transmission. Simultaneous recording of MTS parameters at several points in the body is also possible. The ability to track motion artifacts due to the use of an in-built accelerometer expands the range of functional tests that can be applied. Long-term monitoring of MTS is possible during wakefulness and sleep states. Remote diagnosis of patients can also be performed, improving their level of comfort during measurements. These features make wearable analyzers highly versatile, finding applications in both clinical settings and rehabilitation practices, where they contribute to more accurate and efficient patient treatment.

The aim of this work is to assess the physiological variability and reproducibility of the microcirculatory-tissue systems parameters of the human body across different skin areas, employing wearable multimodal analyzers that implement the LDF and FS methods.

2 | Materials and Methods

The studies were conducted in accordance with the Helsinki Declaration of 2013 by the World Medical Association and approved by the Ethics Committee of Orel State University (Protocol no. 31 of 27-07-2024). All studies were performed at approximately the same time of day to avoid circadian rhythm effects on blood circulation and at a standardized room temperature of 23°C ± 1°C. The research protocol involved the simultaneous recording of LDF and FS signals for 10 min, serving as the baseline recording. Additionally, an occlusion test (OT) was conducted by applying a tonometer cuff to compress the brachial artery with a pressure of 200 mmHg. The OT lasted for 3 min, followed by a recording of perfusion restoration to its initial level for 7 min. During the basal recording (basic test—BT), the volunteers lay supine and during OT were sitting at a table with their hands located on the table at the heart level. Conducting OT with subsequent assessment of parameters such as maximum level of blood flow during post-occlusion hyperemia allows us to evaluate the functional state of small vessels and adaptive reserves of the MTS.

The study included 5 men and 6 women aged 23 ± 3 years old. Blood pressure values for volunteers were 118 ± 7 mmHg for systolic and 78 ± 6 mmHg for diastolic blood pressure, pulse was 80 ± 9 bpm, body mass index 21 ± 3 for women and 23 ± 3 for men. 10 BT measurements were performed for each volunteer and 5 volunteers conducted 6 additional studies with OT. Before starting the study, each volunteer provided their informed consent and completed a questionnaire about their medical history. The exclusion criteria for the study included smoking, the regular use of medication, and the presence of chronic conditions affecting the cardiovascular and endocrinological systems.

A series of experimental studies were conducted utilizing a distributed system of wearable multimodal analyzers LAZMA PF, which implements LDF and FS methods with temperature control and a Bluetooth channel for transferring data to a personal computer. VCSEL lasers operating at a wavelength of 850 nm in the LDF channel and LEDs emitting at 365 nm in the FS channel are employed as radiation sources. The direct illumination of the tissue via a window on the back panel, coupled with the

TABLE 1 | Technical characteristics of the laser Doppler flowmetry systems.

Manufacturer	Perimed AB	LAZMA Ltd.	Transonic Systems Inc.	Moor Instruments Ltd.	Oxford Optronix Ltd.	LEA Medizintechnik
City, country	Stockholm, Sweden	Moscow, Russia	Ithaca, New York, USA	Axminster, UK	Oxford, UK	Giessen, Germany
Wavelength of the radiation sources, nm	632.8, 780	850, 1064	780	633, 785, 830	785 ± 10	760, 830, 850
Power of the radiation sources, mW	2	0.8–1.2	2	1–3	0.5–1	< 30
Source–detector separation (measurement base), mm	0.12–1.5	1–1.2	0.127–0.5	0.2–1.5	0.5 and more	8, 15
Sampling depth, mm	—	1–2	1	0.21–0.39	0.5–1.5	2, 8, 15, 16
Sampling volume, mm^3	—	1–3	1	—	1–1.5	—
Type	Stationary with optical fiber	Stationary with optical fiber; wearable without optical fiber	Stationary with optical fiber	Stationary with optical fiber	Stationary with optical fiber	Stationary with optical fiber
References	[72]	[73]	[74]	[75]	[76]	[77]

TABLE 2 | Technical characteristics of the LAKK-M system and LAZMA PF analyzer.

Parameters	LAKK-M	LAZMA PF
Laser Doppler flowmetry channel		
Wavelength of the radiation source, nm	1064	850
Power of the radiation source, mW	1.2	0.8
Source–detector separation (measurement base), mm	1.0	1.2
Fluorescence spectroscopy channel		
Wavelength of the radiation source, nm	365, 450, 532, and 637	365
Spectral measurement range, nm	285–780	365–375 and 450–460
Irradiation mode	Continuous	Pulse (1 Hz)
Power of the radiation source, mW	3	0.4 (average)
Source–detector separation (measurement base), mm	1.0	2.0
General parameters		
Optical radiation delivery method	Fiber optic probe	Directly (without probe)
Power supply	220 V ± 10%, 50 Hz	3.7 V ± 10%
Operating mode setting time (at least), min	30	10
Continuous operation time (not less than), hour	6	5
Overall dimensions:		
– Diagnostic unit, mm;	300 × 260 × 255	60 × 50 × 30
– Composite light guide probe, not less than, m	2	—
Weight, not more than, kg	7	0.08
PC data transfer interface	USB	Bluetooth

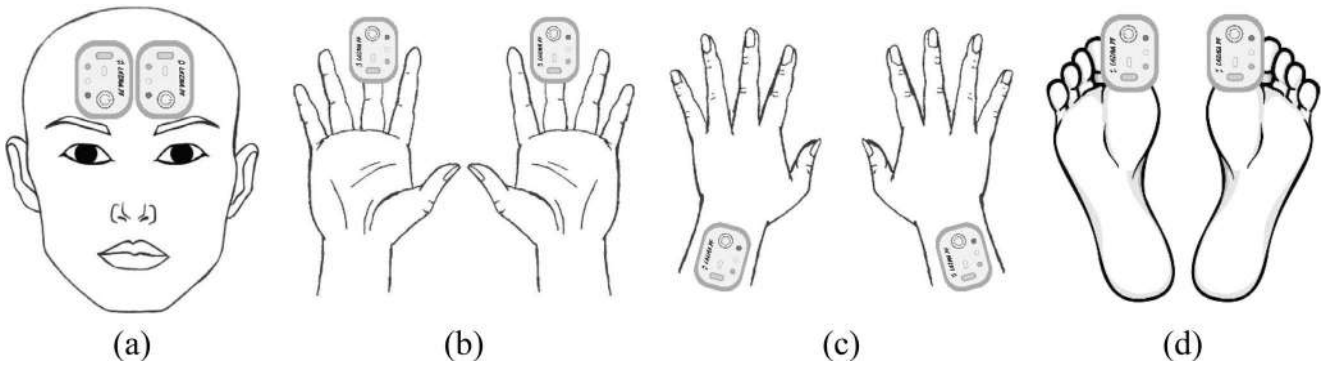

FIGURE 3 | Diagram of measurement areas: Location of the analyzers on forehead (a), fingers (b), wrists (c), and toes (d).

absence of optical fibers, as well as the more convenient attachment to the body, significantly reduces motion artifacts during the measurement process.

During the measurements, the analyzers were placed on the skin of the forehead in the area of supraorbital artery basins (for BT measurements only), the dorsal surface of the upper arms at points located along the medial line 2 cm above the styloid process, the ventral surfaces of the distal phalanges of the third fingers, and the plantar surfaces of the distal phalanges of the first toe (also only for BT measurements). The analyzers were placed symmetrically on both sides of the body. The skin at the points of attachment was cleaned with a disinfectant solution. The exact locations of the analyzers are shown in Figure 3.

Wrists and forehead have non-acral area skin, that has hair, this type of skin covers almost the entire surface of the human body. The surface layers of this type of skin contain a small number of AVA, therefore, blood flow in this area primarily performs a nutritional function [89]. The nervous control of this skin involves both the sympathetic noradrenergic nerves, which constrict blood vessels, and the sympathetic cholinergic nerves, which promote vasodilation [90]. Perfusion values and intravascular pressure in skin microvessels are usually higher in areas

containing AVA (acral areas of fingertips and toes), while areas without AVA have a lower level of blood flow and a higher venous component.

The study of skin hemodynamics in different areas is interesting due to not only the different types of skin in these regions but also because of their morpho-functional characteristics. Perfusion of the supraorbital arteries reflects the blood supply to the brain as the microvessels in this area belong to the internal carotid artery system. In cases of cerebrovascular pathology, this region may serve as a compensatory link between the internal and external carotid arteries. The skin of the fingers and wrists is the most accessible and convenient area for measurement, especially in the case of the application of wearable devices. Vessels in the feet often experience pathological changes first due to the increased stress. Recording MTS parameters in these four regions allows for a comprehensive assessment of the overall function of the MTS in the body both at rest and during functional tests.

Examples of registered signals in the area of supraorbital artery basins are shown in Figure 4 for the right (a, c, e) and left (b, d, f) sides.

In the course of the work, the following MTS parameters were calculated and analyzed:

- I_m is an index of blood microcirculation, characterizing the average level of tissue perfusion with blood per unit of time and measured in perfusion (relative) units;
- Values of the amplitudes of blood flow oscillations in the microcirculatory bed: the amplitude of endothelial oscillations (A_e, 0.0095–0.021 Hz), the amplitude of neurogenic oscillations (A_n, 0.021–0.052 Hz), the amplitude of myogenic oscillations (A_m, 0.052–0.145 Hz), the amplitude of respiratory oscillations (A_r, 0.145–0.6 Hz), the amplitude of cardiac oscillations (A_c, 0.6–2 Hz) [62, 63]. The amplitude value was selected as the maximum extremum of the wavelet spectrum within each frequency range. To obtain the values of the wavelet spectrum, the LDF signal was subjected to a wavelet analysis with a continuous Morlet wavelet [3].
- $A_{460/365}$ is the normalized amplitude of NADH fluorescence. This parameter was calculated using the formula [82, 88]:

$$A_{460/365} = A_{460} / A_{365} \quad (1)$$

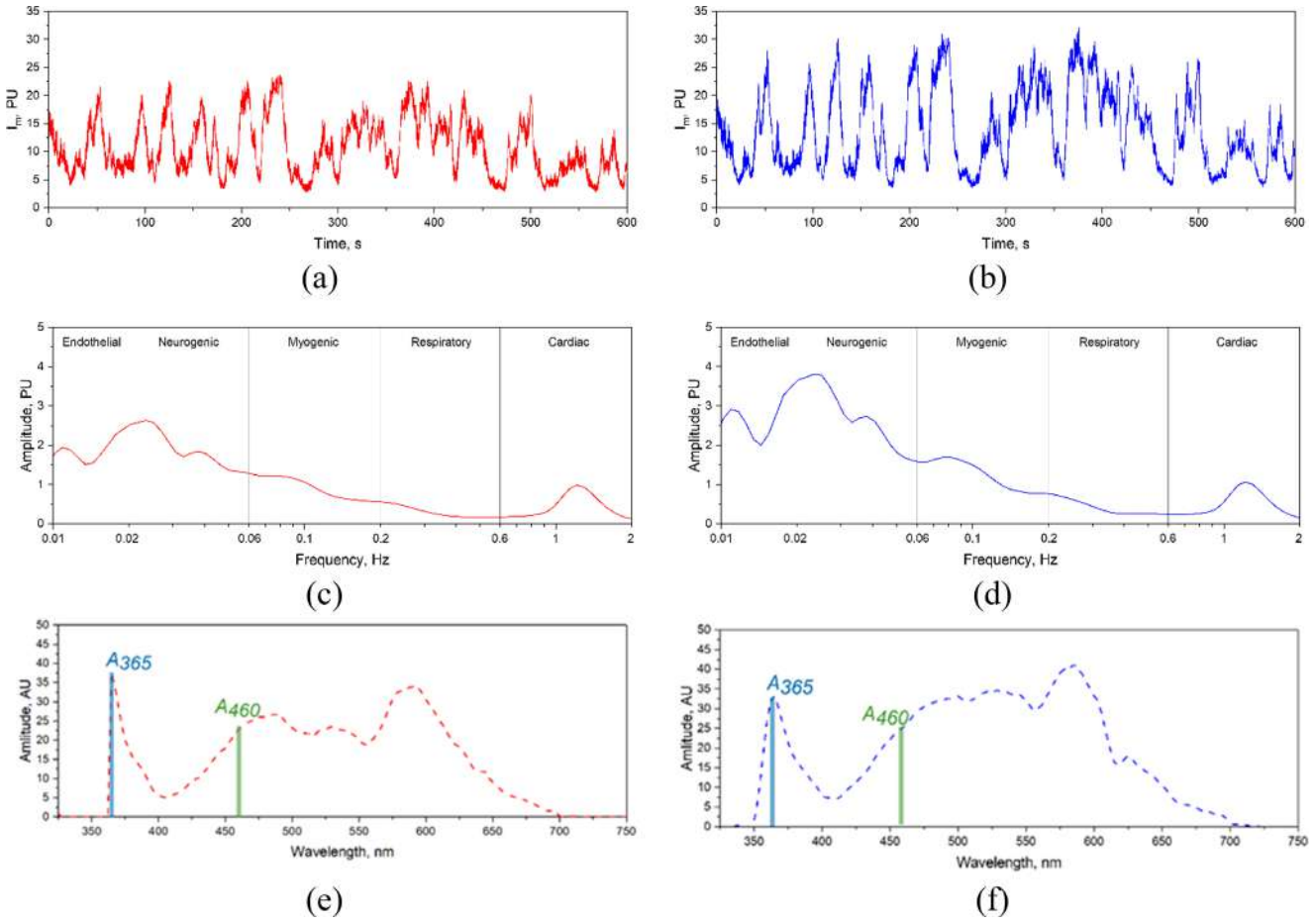

FIGURE 4 | An example of recorded parameters of microcirculatory-tissue systems in the forehead area for the right (a, c, e) and left (b, d, f) sides: Index of microcirculation (a, b), wavelet spectrum of LDF signal (c, d), the fluorescence spectrum* of the skin under excitation of a 365 nm wavelength (e, f) (* full spectra are provided for clarity [measurements were made on a special device with this capability]—wearable devices record the amplitude values of the intensity of back-reflected radiation [highlighted in blue] and the fluorescence peak associated with skin fluorophores—collagen and NADH [highlighted in green]).

where A_{460} is the fluorescence intensity of skin fluorophores at a wavelength of 460 nm, that corresponds to the combined autofluorescence of collagen, elastin and NADH, A_{365} is the intensity of back-reflected radiation at an autofluorescence excitation wavelength of 365 nm (Figure 4e,f). The normalized value of the fluorescence amplitude takes into account the individual optical characteristics of the biotissue. We can hypothesize that during the measurement cycle the content of collagen and elastin in the volunteers' skin has not changed significantly. Therefore, it can be assumed that the parameter $A_{460/365}$ reflects the dynamics of metabolic processes due to changes in the content of NADH coenzyme.

- C_V is the coefficient of variation of MTS parameters;
- I_{m_min}—average perfusion value during occlusion;
- BFR—blood flow reserve, calculated according to occlusion test data [91] Boca Raton.

$$\mathrm{BFR} = \left(\frac{I_{m\_max}}{I_{m\_BT}}\right) \times 100\,\% \tag{2}$$

where I_{m_max} is the maximum perfusion value in the post occlusive reactive hyperemia period (PORH), I_{m_BT} is the average value of perfusion before occlusion.

The C_V was calculated separately for individual MTS parameters of each volunteer, taking as the arithmetic mean the average value of the MTS parameter based on the results of all measurements of this volunteer.

Nutritive blood flow (M_{nutr}) characterizes the capillary part of perfusion, which is directly responsible for the supply of oxygen and essential nutrients to cells through transcapillary exchange. An increase in M_{nutr} (both in absolute units and relative to the overall level of perfusion) is not the goal of microhemodynamics, but a way for the body to respond to an increase in metabolic needs of biological tissues, as well as hyperemia, for example, after occlusion.

To do the calculation of M_{nutr}, the bypass index (BI) parameter was previously calculated using the following formulas [92]. The total value of BI is calculated by adding BI_1 and BI_2. BI_1 represents the shunting index related to differences in tone within the microvessels that carry nutritive and non-nutritive blood flow within the microvascular bed. BI_2 represents the shunting index associated with variability in perfusion of both microvessels and larger vessels (arteries, venules, and veins) during conditions of arterial hyperemia and venous stagnation [93].

$$BI = \frac{A_n}{A_m} \tag{3}$$

where A_n and A_m—respectively maximum amplitudes of oscillations of neurogenic and myogenic frequency ranges (for zones with AVA).

$$BI_1 = \frac{A_{max}}{A_m} \tag{4}$$

where A_{max}—the maximum amplitude of active oscillations (for zones without AVA). BI_2 is calculated in the same way for zones with AVA and without AVA.

$$BI_2 = \frac{A_{c(r)}}{A_m} \tag{5}$$

where $A_{c(r)}$ – the dominant amplitude of oscillations of the heart and respiratory rhythms. It is taken into account if it is greater than or equal to 1. By the calculation of BI, it is possible to assess the perfusion of nutritive and shunt pathways in microvascular networks. In areas with AVA M_{nutr} is calculated by the expression:

$$M_{nutr} = \frac{I_m}{1 + BI} \tag{6}$$

For areas without AVA:

$$M_{nutr} = \frac{I_m}{BI} \tag{7}$$

The shunt blood flow (M_{shunt}) represents the non-nutritive component of perfusion, which is a part of the peripheral blood flow that bypasses the capillary bed through the AVA. The process of shunting blood flow serves as a crucial mechanism for ensuring required, but not excessive, cellular nutrition. Moreover, it acts as a vital protective mechanism for both capillaries and surrounding tissues, particularly against the development of edema. Accordingly, the value M_{shunt} is estimated by the expression:

$$M_{shunt} = I_m - M_{nutr} \tag{8}$$

The oxidative metabolism index (OMI) reflects the consistency of the work of nutrient delivery systems by the bloodstream in the microcirculatory link of the bloodstream, as well as their consumption and utilization of cell waste products. The calculation of OMI is carried out according to the following formula [94]:

$$OMI = \frac{M_{nutr}}{K \times A_{460/365}} \tag{9}$$

where $A_{460/365}$ – the normalized amplitude of NADH fluorescence obtained by dividing the fluorescence intensity at a wavelength of 460 nm by the intensity of the back-reflected radiation at a wavelength of 365 nm; K—the proportionality coefficient.

The intraclass correlation coefficient (ICC) was also calculated for MTS parameters. The ICC shows the reproducibility of data across days for each volunteer. Since the sample consisted of repeated measurements on the same group of volunteers, a two-factor mixed approach, model alpha, type absolute agreement, was selected for the calculation of ICC [95, 96]. ICC values less than 0.5 correspond to poor reproducibility, values 0.5–0.75—moderate reproducibility, values 0.75–0.9—good reproducibility, and values greater than 0.90 indicate excellent reproducibility [95].

The statistical analysis of the data was carried out in the software environment Origin Pro 2021. Due to the limited sample

size, the nonparametric Mann–Whitney *U*-test was used to check the statistical significance of the differences (values of $p < 0.05$ were considered significant). ICC was calculated in IBM SPSS Statistics software.

3 | Results and Discussion

Through the article, the data are presented in the format mean ± standard deviation (SD). In Figures 5–9 the measurement areas to which the diagrams belong indicated schematically, each axis represents one volunteer.

It should be noted that there were no statistically significant differences in the average level of blood microcirculation between the groups of men and women in our study. In all areas of the study, the values of I_m for female and male volunteers were comparable.

Figure 5 shows the coefficients of variation of the index of blood microcirculation for the skin areas of the forehead, fingers and toes, as well as the back of the wrists.

The forehead and finger areas are characterized by similar variability in the blood microcirculation index (25% ± 11% and 24% ± 11% on average, respectively). In the general assessment, the lowest variability of the I_m (18% ± 7%) is observed in the wrist area, which may be due to the lowest perfusion level in relation to other areas of interest due to the anatomical features of this zone (Table 2). In individual assessments, a low coefficient

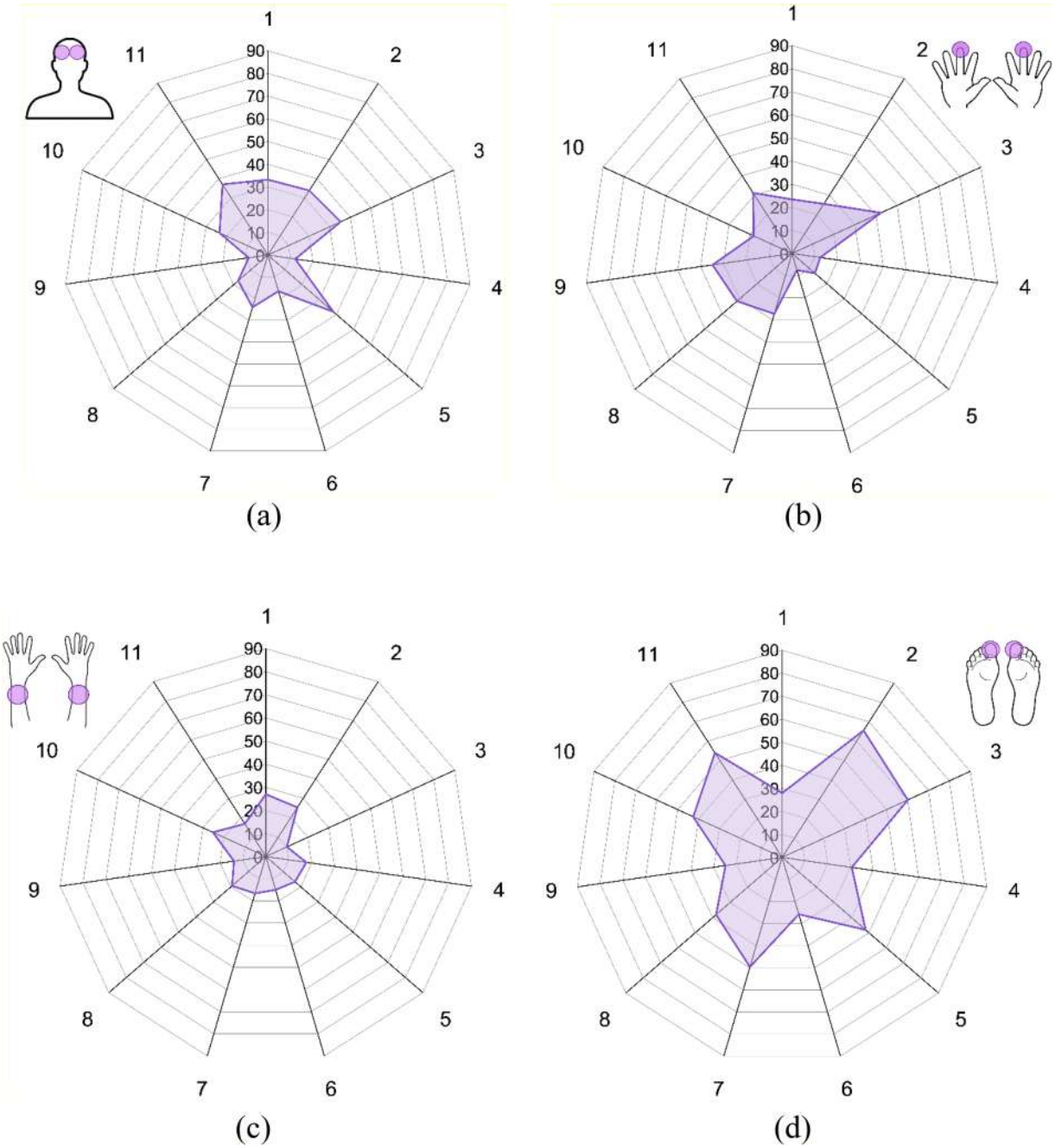

FIGURE 5 | Coefficients of variation (%) of index of blood microcirculation for forehead (a), fingers (b), wrists (c), and toes (d).

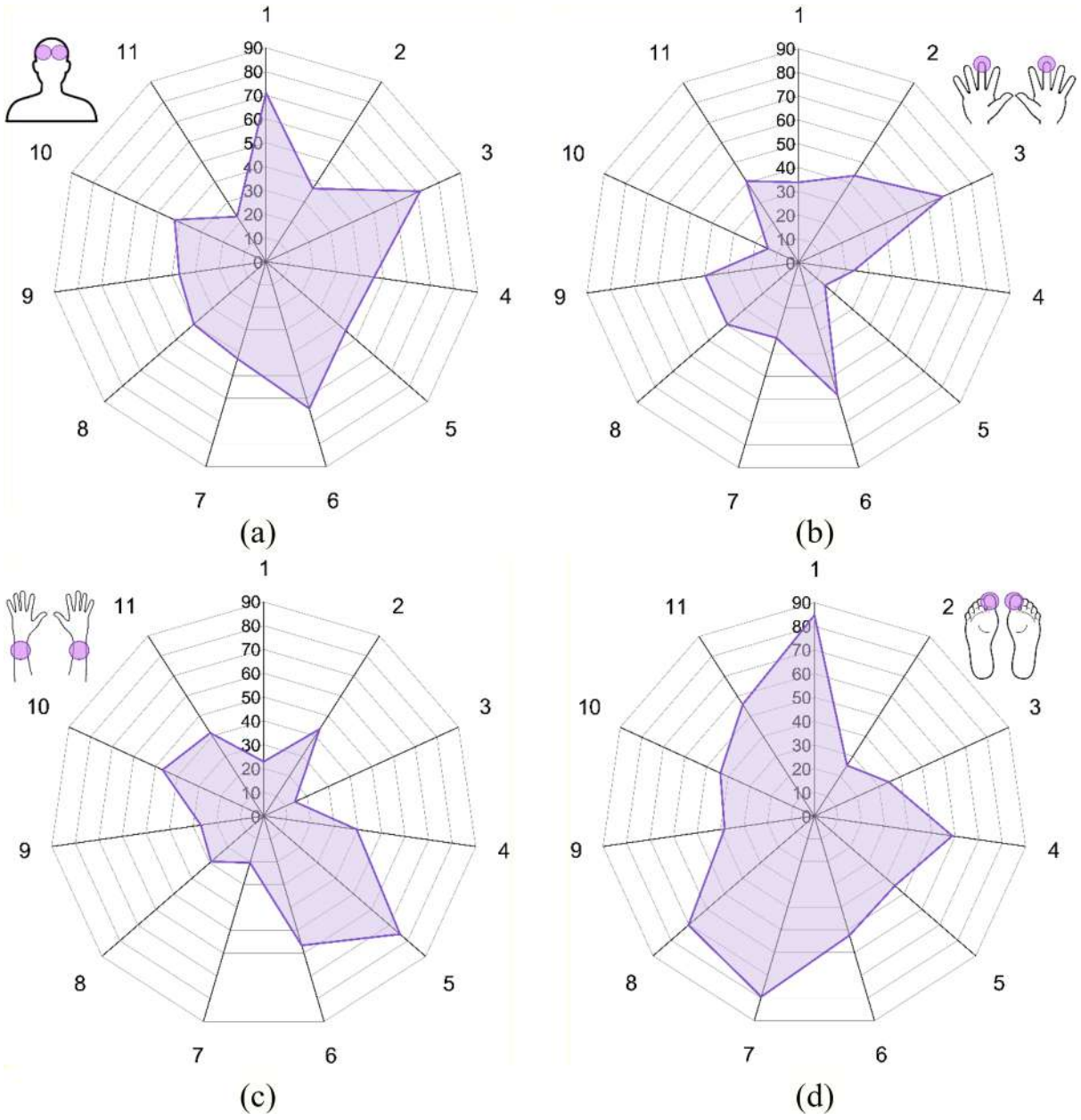

FIGURE 6 | Coefficients of variation (%) of nutritive blood flow for forehead (a), fingers (b), wrists (c), and toes (d).

of variation of I_m was noted in the wrist area for 5 volunteers, in the fingers for 4, and in the forehead for 3. Some volunteers (e.g., numbers 4 and 6) consistently showed low variability, while others (e.g., number 3) had consistently high C_V values. Others displayed mixed results: volunteer 9 had low I_m variability in the forehead and toes but high in the fingers and wrists, while Volunteer 2 had high variability in the forehead and legs but low in the hands. These individual differences should be considered when forming study groups, such as pre-assessing variability to exclude participants with high C_V values.

The toes are characterized by the highest coefficient of variation of the blood microcirculation index—42% ± 14%, and it is in this area that the coefficient of variation of I_m is maximum for 9 out of 11 volunteers. Such values of the C_V may be due to the wearing of shoes, as well as different levels of physical activity on the days of the study. In the future, when measuring the toe area, it will be important to consider various factors such as the number of steps taken, whether sports are involved, the presence or absence of flat feet, and the type of footwear, hosiery, and subjective assessment of shoe comfort.

The average values of the 11 volunteers' microcirculatory-tissues parameters and coefficient of variation for different study areas are presented in Table 3.

ICC showed a good level of reproducibility for almost all areas of the study (more than 0.5), the highest reproducibility was shown by the parameters of A_m and $A_{460/365}$ in the area of wrists, fingers and toes. ICC of I_m and M_{nutr} is also good and excellent (0.7–0.9). However, some values of ICC are below the level of 0.5, for example, A_c in the fingers, I_m, M_{shunt}, and A_r in the toes, which can

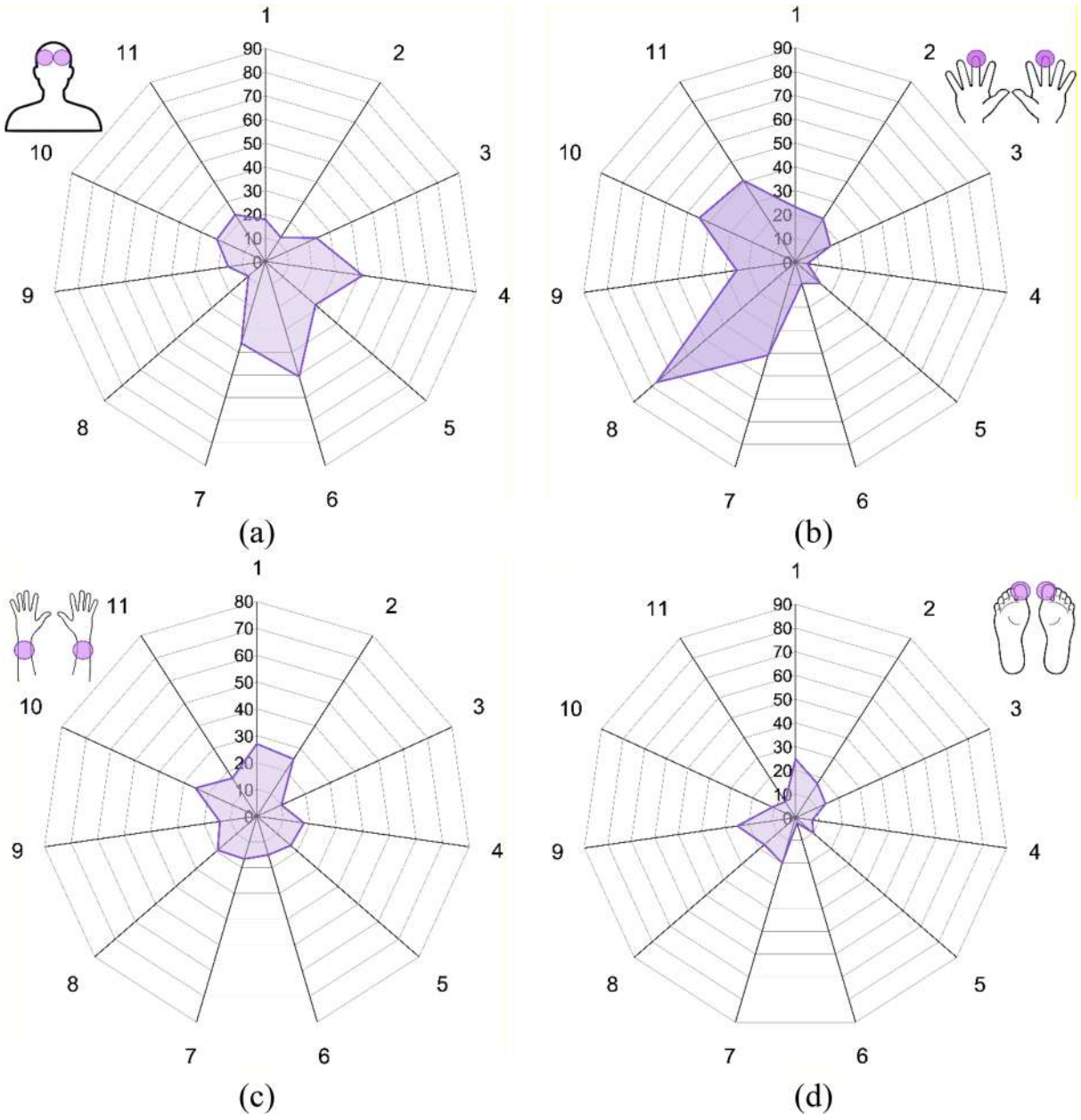

FIGURE 7 | Coefficients of variation (%) of normalized amplitude of NADH fluorescence for forehead (a), fingers (b), wrists (c), and toes (d).

be explained by the angioarchitectonics of the study area (the presence of AVA). The results of reproducibility of the data in the toes are also influenced by shoes and physical activity on the day of measurement, and ICC values for M_{shunt} in toes may be the result of the specifics of data distribution [97].

Figure 6 shows the coefficients of variation of the nutritive blood flow for the skin area of the forehead, fingers and toes, as well as the back of the wrists.

Nutritive blood flow is a calculated parameter that reflects the capillary component of the total blood flow.

The coefficient of variation of nutritive blood flow for a group of 11 volunteers averaged 47% ± 15% for the skin of the forehead, and 53% ± 19% for the toes, which is the highest value. For fingers and wrists, the coefficient of variation was 37% ± 16% and 38% ± 18%, respectively. We can conclude that M_{nutr} has the best reproducibility in the hand area.

When assessing the variability of the M_{nutr} of each volunteer, we can talk about the influence of individual body characteristics on this parameter, differences are observed both within one area of interest between volunteers and for one volunteer between different areas of interest. At the same time, the relationship between the absolute value of M_{nutr} and the variability of this parameter is not observed (Table 2).

Figure 7 shows the coefficients of variation of the normalized amplitude of NADH fluorescence for the skin area of the forehead, fingers and toes, as well as the back of the wrists.

The highest values of the normalized amplitude of NADH fluorescence were noted in the areas of the skin of the forehead

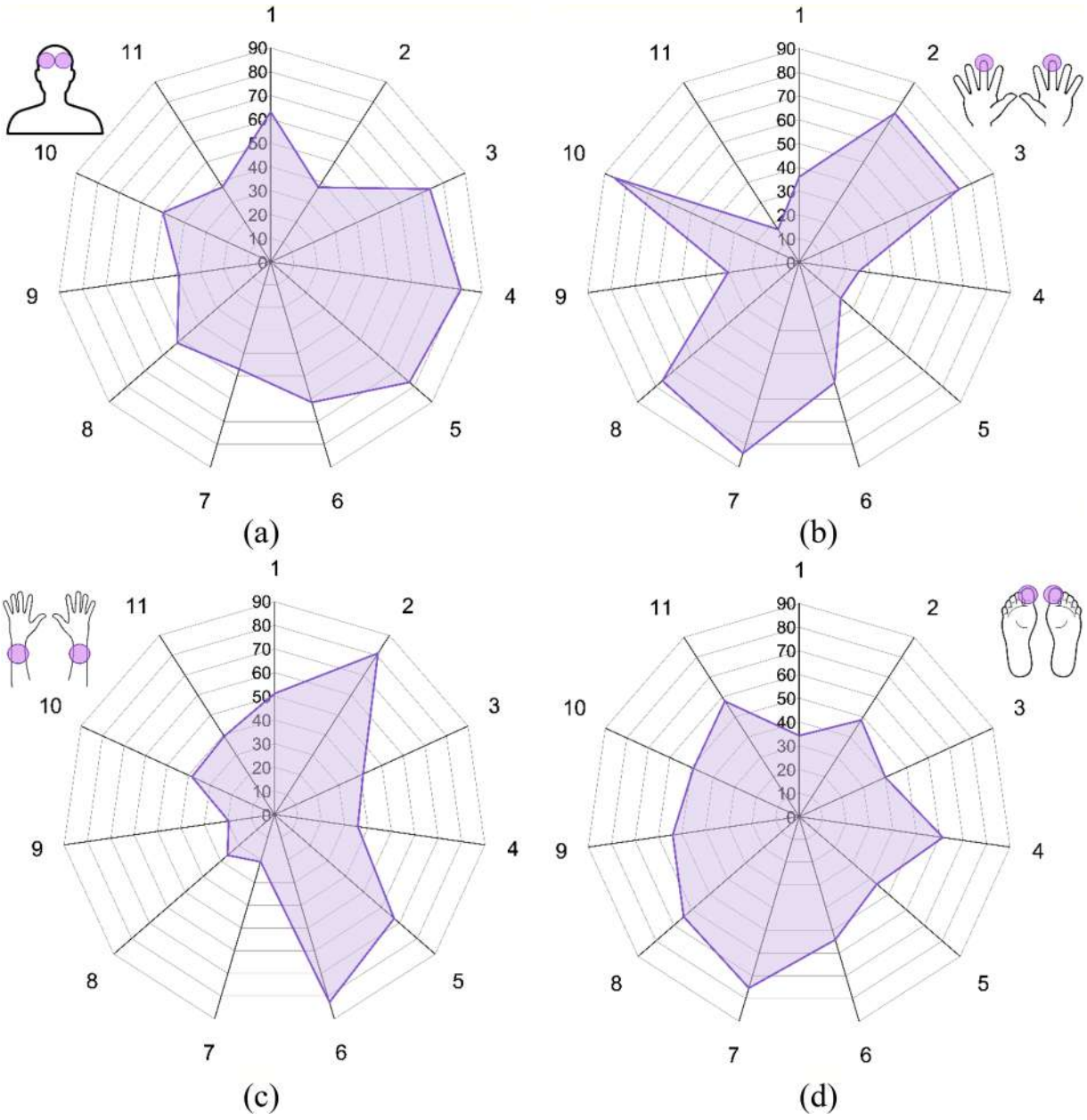

FIGURE 8 | Coefficients of variation (%) of oxidative metabolism index for forehead (a), fingers (b), wrists (c), and toes (d).

and forearms (0.7 ± 0.6 AU and 1.6 ± 0.7 AU, respectively), the lowest value corresponds to the area of the finger and is 1.1 ± 1.0 AU. In the area of the skin of the toes, the value of the normalized amplitude of NADH fluorescence was 0.6 ± 0.2 AU.

The coefficient of variation of the normalized amplitude of NADH fluorescence for a group of 11 volunteers averaged 26% ± 13% for the forehead skin, 14% ± 7% for the toes and 19% ± 5% for the wrist area. The greatest variability of normalized amplitude of NADH fluorescence is observed in the area of the fingers (29% ± 21%), which is facilitated by high values of variability parameters in volunteer no. 8, which may be due to individual characteristics of the body and may occur in a larger number of people with an increase in sample sizes.

Figure 8 shows the coefficients of variation of the oxidative metabolism index for the skin area of the forehead, fingers and toes, as well as the back.

The variability of *OMI* is at the level of 52% on average for all anatomical areas. In the area of the forehead skin, the coefficient of variation was 56% ± 16%, and in fingers and toes 53% ± 27%, and 53% ± 12%, respectively. There is practically no AVA in the wrist area, that is, nutritive blood flow prevails, which may cause a lower variability of *OMI* in this area (46% ± 22%).

It is worth noting that for each area of research, it is possible to divide volunteers into two groups of approximately equal numbers with a high and low degree of variability of the OMI parameter. However, the division will be different for each research area, which is evidence of both the individual characteristics of the volunteers and the anatomical and topographic differences in the selected research areas.

The group variability of the MTS parameters for the right and left sides of the study areas is shown in Figure 9.

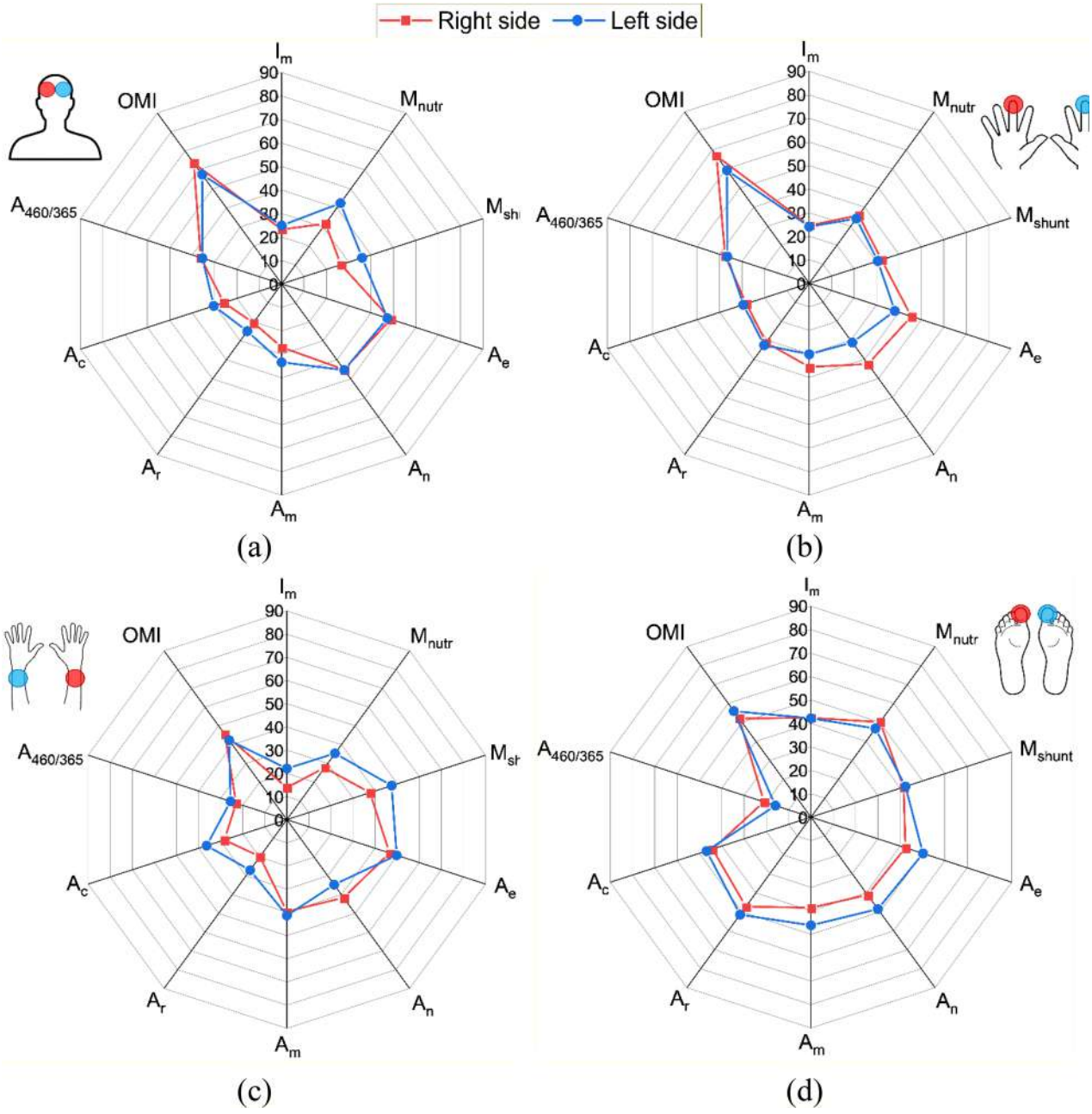

FIGURE 9 | Coefficients of variation (%) of MTS parameters for forehead (a), fingers (b), wrists (c), toes (d) for the right (red) and left (blue) sides of the body.

The lowest variability for all study areas is the average perfusion (I_m) and the normalized amplitude of NADH fluorescence ($A_{460/365}$). This can be explained by the fact that these parameters are measured directly, whereas the oscillation amplitudes of the tonus-forming mechanisms, nutritive and shunt blood flow, as well as *OMI*, are calculated parameters.

In the forehead and upper extremities, the oscillation amplitudes of active regulatory mechanisms (endothelial, neurogenic, and myogenic) have a higher level of variability ($40.2\% \pm 6.9\%$) than the oscillation amplitudes of passive regulatory mechanisms ($27.8\% \pm 4.8\%$). In the leg region, the variability of the amplitudes of fluctuations in microcirculation averaged $45.7\% \pm 4.1\%$. The higher variability characteristic of local mechanisms of regulation of the skin of the forehead and upper extremities can be explained by their primary involvement and operational response to the functional state of the body.

Figure 9 illustrates the good similarity of the variability of MTS parameters (especially for I_m and $A_{460/365}$) on the right and left sides of the measurement, which indicates that the obtained characteristics of MTS parameters variability are caused by physiological features of the skin rather than by measurement peculiarities. The use of functional tests leads to a decrease in the variability of parameters of microcirculatory and tissue systems. The coefficients of variation of microcirculation parameters for the OT are shown in Table 4.

TABLE 3 | Average values of the MTS parameters, coefficient of variation and intraclass correlation coefficient for different study areas.

MTS parameters	Areas of the study									
	Forehead			Wrist			Finger		Toe	
	Mean ± SD	C_V, %	ICC, AU	Mean ± SD	C_V, %	ICC, AU	Mean ± SD	C_V, %	ICC, AU	Mean ± SD	C_V, %	ICC, AU
I_m, PU	18.6 ± 9.0	48.2	0.8	5.1 ± 0.9	16.6	0.8	17.4 ± 5.8	33.4	0.8	10.3 ± 3.1	29.7	0.4
M_{nut}, PU	9.7 ± 5.1	52.0	0.7	2.9 ± 1.3	43.7	0.9	7.6 ± 3.8	50.3	0.8	4.7 ± 1.9	40.4	0.8
M_{shunt}, PU	9.1 ± 5.7	63.1	0.8	2.2 ± 0.8	37.0	0.8	9.8 ± 3.6	37.1	0.8	5.9 ± 1.7	29.6	0.1
A_e, PU	0.6 ± 0.4	66.1	0.4	0.1 ± 0.1	38.1	0.9	0.6 ± 0.4	69.6	0.9	0.8 ± 0.3	37.7	0.5
A_n, PU	0.7 ± 0.6	80.4	0.7	0.2 ± 0.1	27.5	0.7	0.7 ± 0.5	72.5	0.9	1.0 ± 0.5	46.5	0.8
A_m, PU	0.7 ± 0.3	41.4	0.7	0.2 ± 0.1	50.6	0.9	0.6 ± 0.3	48.4	0.9	0.8 ± 0.3	40.4	0.9
A_i, PU	0.4 ± 0.2	51.5	0.7	0.1 ± 0.1	15.3	0.5	0.4 ± 0.1	36.3	0.8	0.3 ± 0.1	27.9	0.3
A_c, PU	0.8 ± 0.2	24.5	0.8	0.2 ± 0.1	20.9	0.7	0.5 ± 0.2	18.0	0.3	1.1 ± 0.4	33.9	0.8
$A_{460/365}$, AU	0.9 ± 0.7	81.6	0.6	1.6 ± 0.6	39.8	0.9	1.1 ± 0.8	73.6	0.9	0.6 ± 0.1	22.2	0.9

In work [87], the variability of skin perfusion in the area of the volar surface of the forearm was assessed using a fiber sensor. The coefficient of variation of skin perfusion averaged 33%. The authors also calculated the coefficients of perfusion variation of different blood flow rates through the capillaries. Thus, the C_V of perfusion for blood velocity less than 1 mm/s was 24%, and for velocity greater than 1 mm/s amounted to 45%. The lower values of variability in the wrist skin in our study may be associated with obtaining information from different diagnostic volumes due to differences in the technical characteristics of the devices [98].

The use of an arterial occlusion test leads to a slowdown in the blood flow rate in the occluded area, therefore, it can be assumed that lower $C_{V\,Im\_min}$ (compared with $C_{V\,Im\_BT}$) was obtained for perfusion of lower blood velocity, as shown in [87]. The authors of the article [86] show a lower variability of the average perfusion of the forearm skin (22%), whereas in the legs this level reached 24%. In our study, the variability of average perfusion in the leg area is also higher than in the forearm skin (42% and 18%, respectively, and in the left forearm area a variability was only 14%). A lower variability of I_m and higher variability of I_{m_max} and *BFR* of the skin of the forearm than the skin of the finger, which we found, was noted in [99], which confirms the influence of topographic and anatomical features of the structure of the skin and microvascular bed on the variability of blood microcirculation parameters.

As for the nutritive blood flow, the authors in the article [84] showed that the variability of the nutritive component of the blood flow obtained as Capillary Blood Cell Velocity using intravital capillary microscopy was 31% in the forearm area, which is slightly less than the coefficient of variation of the nutritive blood flow obtained in our study in the same area (38%).

The article [83] shows the variability of blood microcirculation in the forearm and forehead areas. The authors note a higher reproducibility of the data in the area of the forehead skin, whereas in our study it was the forearms that had lower perfusion variation coefficients (18% compared with 25% for the forehead skin). Such differences could be explained by differences in the technical characteristics of the equipment used: the radiation power of 2 mW at 632.8 nm versus 0.8 mW at 850 nm for our devices.

In the article [82], the authors recorded endogenous autofluorescence spectra for the forearm and finger pads. At a wavelength of 466 nm in the wrist area, the C_V for each volunteer was in the range of 16%–18% and for the finger area—30%–36%. In our work, the coefficient of variation of the NADH fluorescence intensity normalized for back-reflected radiation at a wavelength of 460 nm was in the range from 9% to 26% in the wrist area and in fingers 5%–25% for volunteers with small variation and 41%–44% for 3 volunteers with high variability (excluding abnormal values). The decrease in the C_V in our work is most likely due to a larger sample (11 volunteers vs. 3). The variation differences are linked to normalizing fluorescence data by backscattered radiation, accounting for individual tissue optical properties. Variability in fluorescence parameters between the finger and wrist is due to anatomical features, such as numerous AVAs in the finger and their near

TABLE 4 | Coefficients of variation and intraclass correlation coefficient for blood microcirculation parameters during occlusion test.

	Volunteers no.	I_{m_BT}	I_{m_min}	I_{m_max}	BFR
C_v, %	7	20.8	5.2	11.5	13.5
	8	17.6	13.1	12.7	7.6
	9	11.1	10.7	6.9	8.3
	10	31.7	15.9	11.7	13.6
	11	26.3	12.3	8.6	24.5
Mean ± SD		21.5 ± 7.9	11.4 ± 4.0	10.3 ± 2.4	13.5 ± 6.7
ICC, AU		0.9	0.8	0.8	0.9

absence in the wrist. The authors also note the influence of melanin and varying blood levels on recorded fluorescence spectra.

Variability in MTS parameters reported by other authors is explained by differences in equipment characteristics, such as measurement base [100], source-detector separation [78], wavelength, power, and radiation delivery method (direct contact or optical fiber). The source-detector distance determines the depth of optical radiation penetration and diagnostic volume: greater separation covers deeper skin layers, including larger vascular structures, affecting parameter reproducibility. For example, the source-detector distance in [99] was 0.25 mm, while in our devices it is 1.2 mm, which may explain the differences in results.

It is also worth noting, that not only the technical characteristics of the equipment but also the characteristics of the volunteers (sex and age composition of the sample, body mass index, lifestyle, and the presence of hidden diseases) contribute to changing the variability of blood flow parameters. The authors [101] attribute the low reproducibility of the results to the fact that the menstrual cycle day of the young girls who joined the volunteer group was not taken into account in any way. There were 6 girls in our sample, whose cycle was also not taken into account, which could lead to an increase in the coefficients of variation in the MTS parameters.

Additionally, when evaluating the variability of recorded parameters, it is essential to take into account the impact of other factors. For example, the lifestyle of participants and how it might have changed during the study period, as well as their previous activities before measurement (level of cognitive and physical activity, sleep duration, etc.) before the research, along with the experimental conditions, number and expertise of researchers. The work [13, 102] shows the dependence of both the index of microcirculation and oscillation activity of microvessels on the level of pressure applied to the study area. The pressure from the optical fiber and wearable analyzer differs, and currently, the LAZMA PF pressure is subjectively controlled by the researcher and volunteer, contributing to MTS parameter variability. Additionally, pressure is distributed over a larger area with wearable analyzers due to their larger contact surface compared to the fiber probe.

Different areas of the skin have not only different topographic and anatomical structures but also differ in their optical characteristics. For example, the work [103] illustrates the dependence of the depth of radiation penetration on various blood filling of the skin layers. The melanin content in the skin also affects the diagnostic volume [104, 105], a large amount of which absorbs radiation much more strongly, especially in the ultraviolet range.

Our study involved 11 healthy volunteers of a similar age group. However, the statistical power of the study was increased due to the number of measurements taken on each individual. Nevertheless, given these sample parameters, it would be difficult to generalize the findings to a larger population. To gain a deeper understanding of variability in microvascular parameters in the human body, we need to expand our sample size to include individuals from different age groups and clinical backgrounds. This will allow us to evaluate the impact of disease on microcirculatory dynamics, identify deviations from normal values, and develop new diagnostic tools for clinical use. Despite these limitations, our current study marks the beginning of this line of research. The simultaneous measurement of data from 4 different body locations (8 measurement points) has high clinical potential.

The findings obtained are not only of theoretical importance but also hold significant potential for clinical applications in personalized medicine, rehabilitation, sport, and space medicine. These results allow us to establish a baseline for normal variability in parameters of the MTS that takes into account natural physiological fluctuations in the body and individual characteristics of participants. This is critical for comparing with patients with pathological conditions, as deviations from physiological norms can serve as early indicators of peripheral blood flow disorders and oxidative metabolic abnormalities in tissues. Understanding MTS variability is crucial for evaluating the efficacy of treatments and rehabilitation protocols for patients, as well as assessing the body's response to various stimuli such as stress, exercise, hypoxia, and other environmental factors.

4 | Conclusion

Many factors influence changes in the microcirculatory-tissue systems of the human body, contributing to the spatial and temporal heterogeneity of peripheral blood flow and oxidative metabolism parameters in biological tissues. Studying individual and group variability of these parameters is essential for developing optimal research protocols and ensuring accurate data interpretation.

In this work, for the first time, the physiological variability of human MTS parameters was assessed using wearable LDF and FS analyzers in four body areas: the skin of the forehead (frontal region), the dorsal surface of the forearms, the ventral surface of the distal phalanges of the 3rd fingers, and the plantar surface of the distal phalanges of the 1st toes. Both the average perfusion level, the amplitude of LDF signal oscillations, and skin fluorescence amplitude during basal recording, as well as MTS parameters during the occlusion test, were analyzed.

According to the results of the conducted studies, the values of the parameters I_m and $A_{460/365}$ demonstrate the lowest level of variation in the forearm skin. Amplitudes of perfusion oscillations in the endothelial, myogenic and neurogenic ranges (A_e, A_n, and A_m) have shown the highest values of variation, which may be a consequence of a longer period of their manifestation (and therefore a small number of recorded single oscillations in these frequency ranges during the measurement), and this fact must be considered when analysing the findings of the measurements.

The LDF parameters are characterized by the greatest variability in the toes area—40%–60%. This result may be related to the specifics of the measurement area—despite the fact that before the start of measurements, volunteers were given time to adapt to environmental conditions, wearing shoes and walking prior to measurements could have influenced such a large variability of parameters in this area.

The normalized amplitude of NADH fluorescence is characterized by acceptable values of the coefficient of variation (up to 30%) in the majority of volunteers in the skin areas of the fingers and toes, as well as the forearms.

The parameters obtained using an occlusion test demonstrate high reproducibility (the coefficient of variation in most cases is below 20%), which confirms the advantage of using functional tests to increase the reproducibility of the results of the studies and diagnostic procedures.

Thus, assessing the group variability of the parameters of microcirculatory-tissue systems with wearable analyzers, the lowest C_V for the parameters of peripheral blood flow is observed in the wrist area, and for the parameters of oxidative metabolism—in the area of the toes and wrists. Good reproducibility of data has been obtained for all areas of the research, which increases with the use of occlusion test. Taking into account the difference in technical characteristics and the size of the research samples, we can talk about the comparability of variability for wearable and stationary devices. The described approach allows us to obtain generalized information about the parameters of the microcirculatory-tissue systems throughout the human body and substantiate medical and technical requirements for wearable devices.

Acknowledgments

The work was carried out with the financial support of the Russian Science Foundation (project no. 23-25-00522).

Conflicts of Interest

The authors declare no conflicts of interest.

Data Availability Statement

The data that support the findings of this study are available from the corresponding author upon reasonable request.

References

1. J.-L. Cracowski and M. Roustit, "Human Skin Microcirculation," *Comprehensive Physiology* 10 (2020): 1105.

2. P. C. Johnson, *Overview of the Microcirculation*, (San Diego: Academic Press, 2008), xi–xxiv.

3. E. Zharkikh, Y. Loktionova, and A. Dunaev, "Microcirculatory Dysfunction in Patients With Diabetes Mellitus Detected by a Distributed System of Wearable Laser Doppler Flowmetry Analysers," *Journal of Biophotonics* 17 (2024): e202400297.

4. A. Frolov, Y. Loktionova, E. Zharkikh, V. Sidorov, A. Tankanag, and A. Dunaev, "Effects of Voluntary Changes in Minute Ventilation on Microvascular Skin Blood Flow," *Journal of Science in Sport and Exercise* (2024): 1.

5. G. R. Boss and J. E. Seegmiller, "Age-Related Physiological Changes and Their Clinical Significance," *Western Journal of Medicine* 135 (1981): 434–440.

6. M. D. Cheitlin, "Cardiovascular Physiology? Changes With Aging," *American Journal of Geriatric Cardiology* 12 (2003): 9–13.

7. A. U. Ferrari, A. Radaelli, and M. Centola, "Invited Review: Aging and the Cardiovascular System," *Journal of Applied Physiology* 95 (2003): 2591–2597.

8. L. Li, S. Mac-Mary, J.-M. Sainthillier, S. Nouveau, O. De Lacharriere, and P. Humbert, "Age-Related Changes of the Cutaneous Microcirculation In Vivo," *Gerontology* 52 (2006): 142–153.

9. Y. Wei, H. Jiang, Y. Shi, et al., "Age-Related Alterations in the Retinal Microvasculature, Microcirculation, and Microstructure," *Investigative Ophthalmology & Visual Science* 58 (2017): 3804–3817.

10. L. Li, S. Mac-Mary, D. Marsaut, et al., "Age-Related Changes in Skin Topography and Microcirculation," *Archives of Dermatological Research* 297 (2006): 412–416.

11. I. Bentov and M. J. Reed, "The Effect of Aging on the Cutaneous Microvasculature," *Microvascular Research* 100 (2015): 25–31.

12. M. A. James, J. Tullett, A. G. Hemsley, and A. C. Shore, "Effects of Aging and Hypertension on the Microcirculation," *Hypertension* 47 (2006): 968–974.

13. E. A. Zherebtsov, E. V. Zharkikh, Y. I. Loktionova, et al., "Wireless Dynamic Light Scattering Sensors Detect Microvascular Changes Associated With Ageing and Diabetes," *IEEE Transactions on Biomedical Engineering* 70 (2023): 3073–3081.

14. H. Degens, *Oxygen Transport to Tissue XX* (Boston, MA: Springer US, 1998), 343.

15. J. Grayson, "Responses of the Microcirculation to Hot and Cold Environments," *Pharmacology & Therapeutics* 38 (1988): 201–214.

16. A. Pranskūnas, Ž. Pranskūnienė, E. Belousovienė, et al., "Effects of Whole Body Heat Stress on Sublingual Microcirculation in Healthy Humans," *European Journal of Applied Physiology* 115 (2015): 157–165.

17. C. W. Song, L. M. Chelstrom, S. H. Levitt, and D. J. Haumschild, "Effects of Temperature on Blood Circulation Measured With the Laser Doppler Method," *International Journal of Radiation Oncology, Biology, Physics* 17 (1989): 1041–1047.

18. M. A. Volynsky, N. B. Margaryants, O. V. Mamontov, and A. A. Kamshilin, "Contactless Monitoring of Microcirculation Reaction on Local Temperature Changes," *Applied Sciences* 9 (2019): 4947.

19. P. Van den Brande, A. De Coninck, and P. Lievens, "Skin Microcirculation Responses to Severe Local Cooling," *International Journal of Microcirculation* 17 (1997): 55–60.

20. W. Ren, L. Xu, X. Zheng, F. Pu, D. Li, and Y. Fan, "Effect of Different Thermal Stimuli on Improving Microcirculation in the Contralateral Foot," *Biomedical Engineering Online* 20 (2021): 1.

21. A. S. Popel and P. C. Johnson, "Microcirculation and Hemorheology," *Annual Review of Fluid Mechanics* 37 (2005): 43–69.

22. O. K. Baskurt and H. J. Meiselman, "Blood Rheology and Hemodynamics," *Seminars in Thrombosis and Hemostasis* 29 (2003): 435–450.

23. X. Tao, Y. Chen, K. Zhen, S. Ren, Y. Lv, and L. Yu, "Effect of Continuous Aerobic Exercise on Endothelial Function," *Frontiers in Physiology* 14 (2023): 1043108.

24. L. Streese, C. Guerini, L. Bühlmayer, et al., "Physical Activity and Exercise Improve Retinal Microvascular Health as a Biomarker of Cardiovascular Risk," *Atherosclerosis* 315 (2020): 33–42.

25. N. G. Sidoryak and E. V. Rozova, "Physical Activity and Exercise Improve Retinal Microvascular Health as a Biomarker of Cardiovascular Risk: A Systematic Review," *Bulletin of the Karaganda University "Biology Medicine Geography Series"* 102 (2021): 76.

26. J. L. Greaney, A. Surachman, E. F. H. Saunders, L. M. Alexander, and D. M. Almeida, "Greater Daily Psychosocial Stress Exposure Is Associated With Increased Norepinephrine-Induced Vasoconstriction in Young Adults," *Journal of the American Heart Association* 9 (2020): e015697.

27. J. Gebicki, J. Katarzynska, and A. Marcinek, "Effect of Psychological Stress on Microcirculation Oscillations," *Vascular Health and Risk Management* 19 (2023): 79–82.

28. D. Mikhalchenko, A. Vorobyev, A. Alexandrov, Y. Makedonova, and V. Shkarin, "Microhemodynamic Changes as Indicator of Psychoemotional Stress at Dental Treatment," *Arch Euromed* 10 (2020): 101–103.

29. N. Toda and M. Nakanishi-Toda, "How Mental Stress Affects Endothelial Function," *Pflügers Archiv-European Journal of Physiology* 462 (2011): 779–794.

30. A. Leone and L. Landini, "Vascular Pathology From Smoking," *Current Vascular Pharmacology* 11 (2013): 524–530.

31. H.-A. Lehr, "Microcirculatory Dysfunction Induced by Cigarette Smoking," *Microcirculation* 7 (2000): 367–384.

32. G. Monfrecola, G. Riccio, C. Savarese, G. Posteraro, and E. M. Procaccini, "The Acute Effect of Smoking on Cutaneous Microcirculation Blood Flow in Habitual Smokers and Nonsmokers," *Dermatology* 197 (1998): 115–118.

33. L. N. A. Van Adrichem, S. E. R. Hovius, R. Van Strik, and J. C. Van Der Meulen, "Acute Effects of Cigarette Smoking on Microcirculation of the Thumb," *British Journal of Plastic Surgery* 45 (1992): 9–11.

34. M. Saha, V. Dremin, I. Rafailov, A. Dunaev, S. Sokolovski, and E. Rafailov, "Wearable Laser Doppler Flowmetry Sensor," *Biosensors* 10 (2020): 201.

35. P. Henriksson, Q. Lu, U. Diczfalusy, and A. Freyschuss, "Immediate Effect of Passive Smoking on Microcirculatory Flow," *Microcirculation* 21 (2014): 587–592.

36. Z. Jalali, M. Khademalhosseini, N. Soltani, and A. Esmaeili Nadimi, "Smoking, Alcohol and Opioids Effect on Coronary Microcirculation: An Update Overview," *BMC Cardiovascular Disorders* 21 (2021): 1.

37. V. Linardatou, E. Karatzanos, N. Panagopoulou, et al., "Passive Smoking Acutely Affects the Microcirculation in Healthy Non-Smokers," *Microvascular Research* 128 (2020): 103932.

38. M. H. Smolensky, R. C. Hermida, R. J. Castriotta, and F. Portaluppi, "Role of Sleep-Wake Cycle on Blood Pressure Circadian Rhythms and Hypertension," *Sleep Medicine* 8 (2007): 668–680.

39. Q. Han, Z. Bagi, and R. D. Rudic, "Circadian Clocks and Rhythms in the Vascular Tree," *Current Opinion in Pharmacology* 59 (2021): 52–60.

40. Y.-F. Guo and P. K. Stein, "Circadian Rhythm in the Cardiovascular System," *American Heart Journal* 145 (2003): 779–786.

41. D. P. Veerman, B. P. M. Imholz, W. Wieling, K. H. Wesseling, and G. A. van Montfrans, "Circadian Profile of Systemic Hemodynamics," *Hypertension* 26 (1995): 55–59.

42. G. Yosipovitch, L. Sackett-Lundeen, A. Goon, C. Y. Huak, C. L. Goh, and E. Haus, "Circadian and Ultradian (12 h) Variations of Skin Blood Flow and Barrier Function in Non-Irritated and Irritated Skin—Effect of Topical Corticosteroids," *Journal of Investigative Dermatology* 122 (2004): 824–829.

43. Y. Serin and N. Acar Tek, "Effect of Circadian Rhythm on Metabolic Processes and the Regulation of Energy Balance," *Annals of Nutrition & Metabolism* 74 (2019): 322–330.

44. C. A. Wauschkuhn, K. Witte, S. Gorbey, B. Lemmer, and L. Schilling, "Circadian Periodicity of Cerebral Blood Flow Revealed by Laser-Doppler Flowmetry in Awake Rats: Relation to Blood Pressure and Activity," *American Journal of Physiology-Heart and Circulatory Physiology* 289 (2005): H1662–H1668.

45. N. Nernpermpisooth, S. Qiu, J. D. Mintz, et al., "Obesity Alters the Peripheral Circadian Clock in the Aorta and Microcirculation," *Microcirculation* 22 (2015): 257–266.

46. T. Kubo, S. Fukuda, K. Hirata, et al., "Comparison of Coronary Microcirculation in Female Nurses After Day-Time Versus Night-Time Shifts," *American Journal of Cardiology* 108 (2011): 1665–1668.

47. O. V. Zlobina, S. S. Pakhomii, E. V. Smolina, et al., "Effect of Photoperiod Duration on Microcirculation in the Skin as Assessed Experimentally by Laser Doppler Flowmetry," *Optics and Spectroscopy* 129 (2021): 857–860.

48. L. Ruzek, K. Svobodova, L. J. Olson, O. Ludka, and I. Cundrle, Jr., "Increased Microcirculatory Heterogeneity in Patients With Obstructive Sleep Apnea," *PLoS One* 12 (2017): e0184291.

49. N. Wiernsperger, P. Nivoit, and E. Bouskela, "Obstructive Sleep Apnea and Insulin Resistance," *Clinics* 61 (2006): 253–266.

50. M. Roustit and J.-L. Cracowski, "Assessment of Endothelial and Neurovascular Function in Human Skin Microcirculation," *Trends in Pharmacological Sciences* 34 (2013): 373–384.

51. S. A. Landsverk, P. Kvandal, A. Bernjak, A. Stefanovska, and K. A. Kirkeboen, "The Effects of General Anesthesia on Human Skin Microcirculation Evaluated by Wavelet Transform," *Anesthesia and Analgesia* 105 (2007): 1012–1019.

52. E. Tur, "Physiology of the Skin—Differences Between Women and Men," *Clinics in Dermatology* 15 (1997): 5–16.

53. V. H. Huxley and J. Wang, "Cardiovascular Sex Differences Influencing Microvascular Exchange," *Cardiovascular Research* 87 (2010): 230–242.

54. K. Hattori and W. Okamoto, "Skinfold Compressibility in Japanese University Students," *Okajimas Folia Anatomica Japonica* 70 (1993): 69–77.

55. A. Yamamoto, S. Serizawa, M. Ito, and Y. Sato, "Fatty Acid Composition of Sebum Wax Esters and Urinary Androgen Level in Normal Human Individuals," *Journal of Dermatological Science* 1 (1990): 269–276.

56. M. L. Bartelink, H. Wollersheim, A. Theeuwes, D. Van Duren, and T. Thien, "Changes in Skin Blood Flow During the Menstrual Cycle," *Clinical Science* 78 (1990): 527–532.

57. D. Walmsley and M. J. D. Goodfield, "Evidence for an Abnormal Peripherally Mediated Vascular Response to Temperature in Raynaud's Phenomenon," *Rheumatology* 29 (1990): 181–184.

58. N. W. Shock, "Metabolism and Age," *Journal of Chronic Diseases* 2 (1955): 687–703.

59. H. Massudi, R. Grant, N. Braidy, J. Guest, B. Farnsworth, and G. J. Guillemin, "Age-Associated Changes in Oxidative Stress and NAD+ Metabolism in Human Tissue," *PLOS ONE* 7 (2012): e42357.

60. E. Gitsi, A. Kokkinos, S. Konstantinidou, S. Livadas, and G. Argyrakopoulou, "The Relationship Between Resting Metabolic Rate and Body Composition in People Living With Overweight and Obesity," *Journal of Clinical Medicine* 13 (2024): 5862.

61. A. Johnstone, S. Murison, J. Duncan, K. Rance, and J. Speakman, "Factors Influencing Variation in Basal Metabolic Rate Include Fat-Free Mass, Fat Mass, Age, and Circulating Thyroxine But not Sex, Circulating Leptin, or Triiodothyronine," *American Journal of Clinical Nutrition* 82 (2005): 941–948.

62. T. Oosthuyse and A. N. Bosch, "The Effect of the Menstrual Cycle on Exercise Metabolism," *Sports Medicine* 40 (2010): 207–227.

63. M. Hargreaves and L. L. Spriet, "Skeletal Muscle Energy Metabolism During Exercise," *Nature Metabolism* 2 (2020): 817–828.

64. C. Riva, B. Ross, and G. B. Benedek, "Skeletal Muscle Energy Metabolism During Exercise," *Investigative Ophthalmology & Visual Science* 11 (1972): 936.

65. M. D. Stern, "In Vivo Evaluation of Microcirculation by Coherent Light Scattering," *Nature* 254 (1975): 56–58.

66. A. Stefanovska, M. Bracic, and H. D. Kvernmo, "Wavelet Analysis of Oscillations in the Peripheral Blood Circulation Measured by Laser Doppler Technique," *IEEE Transactions on Biomedical Engineering* 46 (1999): 1230–1239.

67. L. Kralj and H. Lenasi, "Wavelet Analysis of Laser Doppler Microcirculatory Signals," *Frontiers in Physiology* 13 (2023): 1076445.

68. J. R. Lakowicz, *Principles of Fluorescence Spectroscopy* (Boston: Springer, 2006).

69. M.-A. Mycek and B. W. Pogue, *Handbook of Biomedical Fluorescence* (Boca Raton: CRC Press, 2003).

70. F. Bartolomé and A. Y. Abramov, "Mitochondrial Med," in *Probing Mitochondrial Funct*, vol. I (New York: Springer, 2015), 263.

71. V. Rajan, B. Varghese, T. G. van Leeuwen, and W. Steenbergen, "Review of Methodological Developments in Laser Doppler Flowmetry," *Lasers in Medical Science* 24 (2009): 269–283.

72. "Perimed. Our Assessment & Diagnostics Portfolio," https://www.perimed-instruments.com/content/assessment-and-diagnostics/.

73. "LAZMA. Diagnostic Equipment," http://www.lazma.ru/eng/.

74. "Transonic. Life Science Research Solutions for Flow Measurement," https://www.transonic.com/research-blood-flow-measurement.

75. "Moor Instruments. Laser Doppler Monitor," https://www.moor.co.uk/products/monitoring/laser-doppler-monitor/.

76. "Oxford Optronix. OxyFlo Blood Flow Monitors," https://www.oxford-optronix.com/oxyflo-blood-flow-monitors.

77. "LEA Medizintechnik.O2C (Oxygen to See)," http://www.lea.de/eng/indexe.html.

78. I. Fredriksson, M. Larsson, and T. Strömberg, "Measurement Depth and Volume in Laser Doppler Flowmetry," *Microvascular Research* 78 (2009): 4–13.

79. K. Johansson, A. Jakobsson, K. Lindahl, J. Lindhagen, O. Lundgren, and G. E. Nilsson, "Influence of Fibre Diameter and Probe Geometry on the Measuring Depth of Laser Doppler Flowmetry in the Gastrointestinal Application," *International Journal of Microcirculation, Clinical and Experimental* 10 (1991): 219–229.

80. M. Larsson, W. Steenbergen, and T. Stroemberg, "Influence of Optical Properties and Fiber Separation on Laser Doppler Flowmetry," *Journal of Biomedical Optics* 7 (2002): 236–243.

81. E. V. Zharkikh, Y. I. Loktionova, A. A. Fedorovich, A. Y. Gorshkov, and A. V. Dunaev, "Assessment of Blood Microcirculation Changes After COVID-19 Using Wearable Laser Doppler Flowmetry," *Diagnostics* 13 (2023): 920.

82. A. V. Dunaev, V. V. Dremin, E. A. Zherebtsov, et al., "Individual Variability Analysis of Fluorescence Parameters Measured in Skin With Different Levels of Nutritive Blood Flow," *Medical Engineering & Physics* 37 (2015): 574–583.

83. S. Sundberg, "Acute Effects and Long-Term Variations in Skin Blood Flow Measured With Laser Doppler Flowmetry," *Scandinavian Journal of Clinical and Laboratory Investigation* 44 (1984): 341–345.

84. A. Houben, D. W. Slaaf, F. C. Huvers, P. W. De Leeuw, A. C. N. Kruseman, and N. C. Schaper, "Diurnal Variations in Total Forearm and Skin Microcirculatory Blood Flow in Man," *Scandinavian Journal of Clinical and Laboratory Investigation* 54 (1994): 161–168.

85. A. V. Dunaev, V. V. Sidorov, N. A. Stewart, S. G. Sokolovski, and E. U. Rafailov, "Laser Reflectance Oximetry and Doppler Flowmetry in Assessment of Complex Physiological Parameters of Cutaneous Blood Microcirculation," in *Advanced Biomedical and Clinical Diagnostic Systems XI* (Bellingham: SPIE, 2013), 27–35.

86. H. Jonasson, I. Fredriksson, A. Pettersson, M. Larsson, and T. Strömberg, "Oxygen Saturation, Red Blood Cell Tissue Fraction and Speed Resolved Perfusion—A New Optical Method for Microcirculatory Assessment," *Microvascular Research* 102 (2015): 70–77.

87. T. Strömberg, F. Sjöberg, and S. Bergstrand, "Temporal and Spatiotemporal Variability in Comprehensive Forearm Skin Microcirculation Assessment During Occlusion Protocols," *Microvascular Research* 113 (2017): 50–55.

88. V. V. Sidorov, Y. L. Rybakov, V. M. Gukasov, and G. S. Evtushenko, "A System of Local Analyzers for Noninvasive Diagnostics of the General State of the Tissue Microcirculation System of Human Skin," *Biomedical Engineering* 55 (2022): 379–382.

89. E. G. Salerud, T. Tenland, G. E. Nilsson, and P. A. Oberg, "Rhythmical Variations in Human Skin Blood Flow," *International Journal of Microcirculation, Clinical and Experimental* 2 (1983): 91–102.

90. J. M. Johnson and D. L. Kellogg, Jr., "Local Thermal Control of the Human Cutaneous Circulation," *Journal of Applied Physiology* 109 (2010): 1229–1238.

91. M. Roustit, and J.-L. Cracowski, "Non-Invasive Assessment of Skin Microvascular Function in Humans: An Insight Into Methods," *Microcirculation* 19 (2012): 47–64.

92. A. V. Dunaev, V. V. Sidorov, A. I. Krupatkin, et al., "Investigating Tissue Respiration and Skin Microhaemocirculation Under Adaptive Changes and the Synchronization of Blood Flow and Oxygen Saturation Rhythms," *Physiological Measurement* 35 (2014): 607–621.

93. A. I. Krupatkin, "Evaluation of the Parameters of Total, Nutritive, and Shunt Blood Flows in the Skin Microvasculature Using Laser Doppler Flowmetry," *Human Physiology* 31 (2005): 98–102.

94. A. Dunaev, "Wearable Devices for Multimodal Optical Diagnostics of Microcirculatory-Tissue Systems: Application Experience in the Clinic and Space," *Journal of Biomedical Photonics and Engineering* 9 (2023): 20201.

95. T. K. Koo and M. Y. Li, "A Guideline of Selecting and Reporting Intraclass Correlation Coefficients for Reliability Research," *Journal of Chiropractic Medicine* 15 (2016): 155–163.

96. P. E. Shrout and J. L. Fleiss, "Intraclass Correlations," *Psychological Bulletin* 86 (1979): 420–428.

97. R. Muller and P. Buttner, "A Critical Discussion of Intraclass Correlation Coefficients," *Statistics in Medicine* 13 (1994): 2465–2476.

98. E. Zharkikh, Y. Loktionova, A. Fedorovich, A. Gorshkov, and A. Dunaev, "Changes in Blood Flow Oscillations Associated with COVID-19 as Measured by Wearable Laser Doppler Flowmetry," In *European Conferences on Biomedical Optics*, (Washington: Optica Publishing Group, 2023), 126272E.

99. M. Roustit, S. Blaise, C. Millet, and J. L. Cracowski, "Reproducibility and Methodological Issues of Skin Post-Occlusive and Thermal Hyperemia Assessed by Single-Point Laser Doppler Flowmetry," *Microvascular Research* 79 (2010): 102–108.

100. A. V. Dunaev, E. A. Zherebtsov, D. A. Rogatkin, N. A. Stewart, S. G. Sokolovski, and E. U. Rafailov, "Substantiation of Medical and Technical Requirements for Noninvasive Spectrophotometric Diagnostic Devices," *Journal of Biomedical Optics* 18 (2013): 107009.

101. C. Millet, M. Roustit, S. Blaise, and J. L. Cracowski, "Comparison Between Laser Speckle Contrast Imaging and Laser Doppler Imaging to Assess Skin Blood Flow in Humans," *Microvascular Research* 82 (2011): 147–151.

102. I. A. Mizeva, E. V. Potapova, V. V. Dremin, et al., "Optical Probe Pressure Effects on Cutaneous Blood Flow," *Clinical Hemorheology and Microcirculation* 72 (2019): 259–267.

103. E. V. Zharkikh, V. V. Dremin, and A. V. Dunaev, "Sampling Volume Assessment for Wearable Multimodal Optical Diagnostic Device," *Journal of Biophotonics* 16 (2023): e202300139.

104. V. V. Dremin and A. V. Dunaev, "How the Melanin Concentration in the Skin Affects the Fluorescence-Spectroscopy Signal Formation," *Journal of Optical Technology* 83 (2016): 43.

105. D. Viktor, G. Nadezhda, P. Elena, and D. Andrey, "Influence of Melanin Content on Laser Doppler Flowmetry and Tissue Reflectance Oximetry Signal Formation," *J. Biomed. Photonics Eng* 7 (2021): 40306.